

THE
PHYSICAL REVIEW

THE SPECTRUM OF BARIUM HYDRIDE

BY W. R. FREDRICKSON, SYRACUSE UNIVERSITY
AND WILLIAM W. WATSON, YALE UNIVERSITY

(Received January 8, 1932)

ABSTRACT

A BaH band system in the region 6925A to 6380A has been photographed with a 21-foot grating (dispersion = 2.04A per mm), using a metallic barium arc in a hydrogen atmosphere at reduced pressure as a source. The spectrum consists of the (0, 0), (1, 1) and (2, 2) bands only, and the analysis of the (0, 0) band shows the system to be the expected ${}^2\Pi \rightarrow {}^2\Sigma$ case *a* type with twelve branches in each band. Assignments of the frequencies to these branches are presented, together with the principal combination differences. The Λ -type doubling is large in the ${}^2\Pi_{1/2}$ state, but small and of opposite sign in the ${}^2\Pi_{1/2}$ state, giving $p_0 = +0.85$ and $q_0 = +0.0067$. The spin doubling in the ${}^2\Sigma$ state is regular, with $\gamma_0 = +0.186$. Other constants are $B_0'' = 3.404$, $D_0'' = -9.61 \times 10^{-5}$, $r_0'' = 2.22 \times 10^{-8}$ cm, $B_{0,-1/2}' = 3.4468$, $D_{0,-1/2}' = -1.13 \times 10^{-4}$, $B_{0,+1/2}' = 3.5156$, and $D_{0,+1/2}' = -1.20 \times 10^{-4}$. The separation of the two ${}^2\Pi$ sublevels yields $A = 462$. The smallness of this value ($A = 832$ for lowest 3P levels of Ba) indicates that this state is possibly formed from a combination of the lowest 3P and 3D states of the Ba atom. A large perturbation in one of the ${}^2\Pi_{1/2a}$ levels, and the sign and magnitude of the p_0 and q_0 , indicate another lower-lying excited level.

INTRODUCTION

THE band spectra which have so far been reported and analysed for diatomic hydrides of all the elements in the second column of the periodic table with the exception of Sr, Ba, and of course Ra involve transitions from excited ${}^2\Pi$ and ${}^2\Sigma$ states to a normal ${}^2\Sigma^+$ state.¹ Among the ${}^2\Pi \rightarrow {}^2\Sigma$ bands are examples of all types of coupling in the ${}^2\Pi$ states from almost strictly case *b* for BeH ($A = 1.97$, $B = 10.3$), with thus only three branches in each band except for a barely resolvable doubling in each branch at the origin, to complete case *a* for HgH ($A = 3683$, $B = 6.58$) with a resulting twelve-branch structure for the bands. For the occurrence of twelve strong branches it is necessary for the doubling of the levels in the ${}^2\Sigma$ state to be appreciable in order that the satellite ${}^PQ_{12}$, ${}^RQ_{12}$, ${}^PQ_{21}$ and ${}^RQ_{21}$ branch lines be separated from the main-branch lines. The known ${}^2\Sigma$, ${}^2\Sigma$ bands for these molecules also display many variations attributable to resonance and perturbing effects on the upper states by other near-lying electronic levels.

¹ The references for the data for these bands, together with discussion of their characteristics, are given by R. S. Mulliken, Phys. Rev. **32**, 388 (1928); **33**, 507 (1929), and R. S. Mulliken and A. Christy, Phys. Rev. **38**, 87 (1931).

It was to be expected then that any ${}^2\Pi \rightarrow {}^2\Sigma$ band systems from the molecules SrH and BaH should contain twelve branches in each band and with fairly large spacing between the ${}^2\Pi_{1/2}$ and ${}^2\Pi_{3/2}$ origins, since the constant A for the coupling between Λ and S could be expected to be almost as large as that for the 3P states of Sr and Ba respectively. Furthermore, judging from the position of the corresponding bands for the other like molecules, it could be predicted that these bands should be found in the red region of the spectrum, near the lowest ${}^3P - {}^3S$ atomic lines. And since the electronic configurations of Ca, Sr, and Ba in the lowest levels are so similar, it was thought that a ${}^2\Sigma, {}^2\Sigma$ transition should lie very near to the ${}^2\Pi \rightarrow {}^2\Sigma$ for SrH and BaH as in the case of CaH, but possibly exhibiting still larger doublings due to the l -uncoupling phenomenon. Precisely this situation has been found to exist in the spectrum of SrH which is described in detail in the following paper. The present paper discusses the spectrum of BaH, which consists principally only of the ${}^2\Pi \rightarrow {}^2\Sigma$ system, but with strong indications of another band system too far into the red to be photographed.

EXPERIMENTAL PROCEDURE

As a source a 110-volt d.c. arc carrying 3 amperes between an anode made of a small piece of metallic barium and a thin flat piece of copper as the cathode was used. This arc was operated in the modified Back chamber mounted between the poles of a large Weiss electromagnet which happened to be in position in front of the slit of the spectrograph. The barium electrodes were about $6 \times 6 \times 4$ mm in size carried at the end of a short length of tungsten wire. Hydrogen at about 5 cm pressure was pumped slowly through the arc chamber during the exposure. It was found that the molecular spectrum was emitted much more strongly from a continuous arc than from the intermittent form of arc employed in the Zeeman effect work. The consumption of four of these small pieces of Ba in the arc sufficed to give intense spectrograms of the BaH bands at the red end in the dicyanine region.

The spectrograms were obtained in the second order of a 21-foot concave grating in a stigmatic mounting, the dispersion being about 2.04Å per mm. A very strong band system, which the analysis given below shows to be a ${}^2\Pi \rightarrow {}^2\Sigma$ transition for BaH, in the near red between 6380Å and 6925Å is emitted by this source. Eastman panchromatic plates dyed with dicyanine to give greater sensitivity at the long wave-length end were used. Fig. 1 is a reproduction of this band system. In addition to these bands, this arc emits a molecular spectrum in the green and yellow regions of the visible spectrum consisting of a considerable density of lines with but little evidence of regularity. This system is perhaps analogous to a ${}^2\Sigma, {}^2\Sigma$ band system for CaH recently partly analysed by Grundström,² and will be investigated later. There is also strong evidence for the existence of another band system still farther into the near infrared, but a spectrogram in the first order taken with a neocyanine-dyed plate fails to reveal it.

² B. Grundstrom, *Zeits. f. Physik* **33**, 235 (1931).

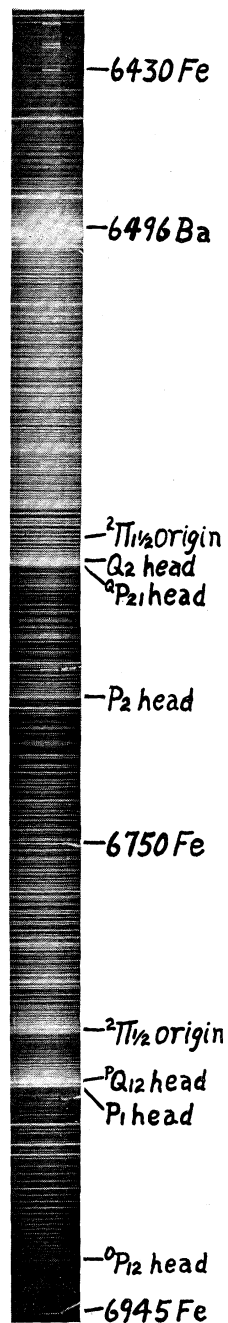


Fig. 1. Reproduction of the $^2\Pi$, $^2\Sigma$ BaH band lying between 6380Å and 6925Å. Note the considerable spacing between the heads of the satellite and main branches, and their equal intensity.

DETAILS OF THE ${}^2\Pi \rightarrow {}^2\Sigma$ BAND

The (0,0), (1,1), and (2,2) bands are present in this system, and analysis of the (0,0) bands reveals twelve branches in a band. In Fig. 1 the double-headed appearance of the band due to the turning of the P_1 and ${}^P Q_{12}$ branches can be seen. Since it is known that the separation of these branches is due to the doubling of the levels of the ${}^2\Sigma$ state and that the separation of the lines having the same K values should be proportional to $K + \frac{1}{2}$, it was at once possible to assign J values to the lines of these series. A similar procedure was employed in determining the Q_1 and ${}^Q R_{12}$, ${}^Q P_{21}$ and Q_2 , and ${}^R Q_{21}$ and R_2 branches. The other series were found by applying various internal combinations which can be determined from an energy level diagram for a ${}^2\Pi \rightarrow {}^2\Sigma$ transition.^{3,4} All series are regular with the exception of a perturbation in the

TABLE I. Assignment of lines for the (0, 0) band of ${}^2\Pi \rightarrow {}^2\Sigma$ system of BaH (cm⁻¹ units; b indicates a broad line due to the fusion of two or more lines; A an atomic line).

$J'' + \frac{1}{2}$	${}^0 P_{12}$	P_1	${}^2\Pi_{1/2} \rightarrow {}^2\Sigma$ ${}^P Q_{12}$	Q_1	${}^Q R_{12}$	R_1
1			14625.82	14633.17	14637.76	14642.83
2		14625.43	22.36	37.24	41.98	52.30
3		21.90	19.21	41.29	46.35	62.39
4		18.50	16.20	45.74	51.01	72.76
5	14586.35	15.32	13.42	50.25	55.81	83.33
6	77.83	12.47	10.79	54.98	60.78	694.06
7	69.69	09.68	08.60	59.89	66.54	705.09
8	61.30	07.04	06.34	65.10	72.09	16.20
9	53.40	04.46	04.46	70.41	77.80	27.52
10	45.77	02.70	02.70	76.01	83.67	38.89
11	38.35	14600.77	01.32	81.63	89.76	50.65
12	31.12	14599.16	14600.13	87.46	14695.95	62.45
13	24.22	97.80	14599.23	93.58	14702.41	74.40
14	17.49	96.63	98.35	14699.79	08.78	86.44
15	11.09	95.63	97.88	14706.24	15.76	14798.88
16	14504.83	94.92	97.58	12.77	22.57	14811.31
17	14498.86	94.50	97.20	19.58	29.57	23.94
18	93.16	94.00	97.52	26.43	37.11	36.74
19	87.73	94.21	98.04	33.59	44.59	49.70
20	82.58	94.42	98.70	40.89	52.23	62.83
21	77.77	94.92	99.61	48.37	59.99b	76.09
22	73.15	95.63	00.86	55.97	67.96b	14889.39
23	68.79	96.63	02.19	63.74	76.02	14902.87
24	64.74	97.80	03.80	71.72	84.41	16.42
25	60.97	14599.16	05.64	79.86	14792.69	30.29
26	57.46	14600.86	07.55	87.98	14801.57	44.50
27	54.09	02.70	09.68	14796.67	10.48	58.23
28	51.42	04.46	12.47	14805.29	19.30	72.12
29	48.81	07.09	15.30	14.15	28.68	14986.49
30	46.51	09.68	18.44	23.07	37.62	15000.67
31	44.42	13.42		32.13	46.85b	
32	42.71	16.20		41.25	55.85	
33	41.26	19.21		50.49		
34	39.93					

³ The energy diagram for HgH given by R. S. Mulliken (Reviews of Modern Physics 3, 130 (1931)) could well represent the facts for BaH by choosing a suitable scale.

⁴ One of the internal combinations used is:

$$\begin{aligned} Q_1(J) - {}^0 P_{12}(J+1) &= R_1(J) - {}^P Q_{12}(J+1) = {}^S R_{21}(J) - Q_2(J+1) \\ &= {}^R Q_{21}(J) - P_2(J+1) = F_2''(J+1) - F_1''(J). \end{aligned}$$

This one combination involves eight of the twelve branches.

TABLE I. (Continued).

$J'' + \frac{1}{2}$	P_2	${}^oP_{21}$	${}^2\Pi_{1/2} \rightarrow {}^2\Sigma$ Q_2	${}^RQ_{21}$	R_2	${}^S R_{21}$
1					15092.20	15098.69
2			15078.32	15091.50	96.19	15109.90
3		15077.72	75.94	95.51	15100.65	20.44
4	15048.96	75.94	73.94	99.95	05.47b	31.74
5	40.59	73.38	72.26	15104.75	10.94b	43.41
6	32.29	71.38	70.92	09.90	16.39	55.64
7	24.26	69.76	70.35b	15.51b	22.54	67.98
8	16.63	68.62	69.39	21.19	28.77	80.69
9	09.53	67.85	68.99	27.14	35.51	15193.76
10	15002.53	67.39	69.12	33.50	42.38	15207.11
11	14996.06	67.01	69.45	40.42	52.17	20.67
12	89.80	67.38	70.16	50.43b	58.00b	34.55
13	86.79	67.85	71.29	55.41	65.53	48.77
14	79.21	68.73	72.82	61.97	73.71	63.29
15	74.22	70.00	74.59	71.03	82.22	78.03
16	69.59	71.38	76.67	79.36	15191.17	15293.01
17	65.46	73.94	79.15	87.95	15200.26	15308.23
18	61.63	75.84	81.90	15196.94	09.53	23.68
19	58.23	78.50	84.98	15206.17	19.34	39.42
20	55.26	81.40	88.42	15.79	29.37	55.43b
21	52.37	84.68	92.20	25.55	39.63	71.49
22	50.15	88.42	15096.19	35.54	50.11	15388.00A
23	48.32	92.20	15100.65	45.94	60.88	15404.46
24	46.89	15096.19	05.43	56.59	71.91	20.90A
25	45.75	15100.65	10.39	67.41	83.21	38.13
26	44.95	05.45b	15.51	78.68	15294.71	55.19
27	44.47	10.94b	21.19	15289.82	15306.48	72.40
28	44.47	16.29	27.14	15301.41	18.27	15489.72
29	44.95	22.07	33.34	13.27	30.65	15507.30
30	45.75	27.52	39.86	25.09	43.01	25.10
31	46.89		46.68	37.56	55.43	42.92
32	48.32		53.64	49.97	68.51	61.02
33	50.15		61.03	62.65	81.34	
34	52.37		68.56	75.55	15394.75	
35	55.26		76.31	15388.77	15408.04	
36			84.53	15401.84	21.62	
37			93.15	15.22	35.23	
38				28.82	49.37	
39				56.31	63.08	
40				70.31	77.19	
41				84.29	91.38	

P_2 , R_2 , and ${}^RQ_{12}$ branches due to a perturbation of the ${}^2\Pi_{1/2d}$ levels around $J'' = 11\frac{1}{2}$. The frequencies of the lines of the twelve branches of the (0,0) band are listed in Table I.

In addition to forming a test of the correctness of the assignments of the band lines to the several branches, the combination differences also serve in the calculation of the molecular constants. The following combinations involving the terms of the lower state may be verified with the aid of the energy level diagram:

$$\begin{aligned} R_1(J-1) - P_1(J+1) &= {}^S R_{21}(J-1) - {}^o P_{21}(J+1) \\ &= F_1''(J+1) - F_1''(J-1) = \Delta_2 F_1''(J) \end{aligned}$$

and

$$\begin{aligned} R_2(J-1) - P_2(J+1) &= {}^o R_{12}(J-1) - {}^o P_{12}(J+1) \\ &= F_2''(J+1) - F_2''(J-1) = \Delta_2 F_2''(J). \end{aligned} \quad (1)$$

These combinations for this BaH band are listed in Table II. The $\Delta_2 F_1''(J)$ values are slightly larger than the $\Delta_2 F_2''(J)$ due to the spin doubling in the ${}^2\Sigma$ state. The last column of the table gives the average of the four combination values, and is the one from which the constants are calculated (cf. next section).

TABLE II. *Lower state combinations.* The 1st set of data gives the $\Delta_2 F_1''(J)$ values obtained from Eq. (1); the second set, the $\Delta_2 F_2''(J)$. The J values have been omitted in headings; $R_1 - P_1 = R_1(J-1) - P_1(J+1)$, etc. The $\Delta_2 F''(K)$ values in the last column are the average of $\Delta_2 F_1''(J=K+\frac{1}{2})$ and $\Delta_2 F_2''(J=K-\frac{1}{2})$, used in Eq. (3).

$J'' + \frac{1}{2}$	$\Delta_2 F_1''(J)$			$J'' + \frac{1}{2}$	$\Delta_2 F_2''(J)$			K	$\Delta_2 F''(K)$
	$R_1 - P_1$	${}^sR_{21} - {}^qP_{21}$	Av.		$R_2 - P_2$	${}^qR_{12} - {}^oP_{12}$	Av.		
2	20.93	20.97	20.95					1	20.95
3	33.80	33.96	33.88					2	33.88
4	47.07	47.06	47.06	4	60.06	60.00	60.03	3	47.06
5	60.29	60.36	60.33	5	73.18	73.18	73.18	4	60.18
6	73.65	73.65	73.65	6	86.68	86.12	86.40	5	73.42
7	87.02	87.00	87.01	7	99.76	99.48	99.62	6	86.70
8	100.63	100.63	100.63	8	113.01	113.14	113.07	7	100.12
9	113.50	113.30	113.40	9	126.24	126.32	126.28	8	113.23
10	126.75	126.75	126.75	10	139.45	139.45	139.45	9	126.51
11	139.73	139.73	139.73	11	152.58	152.55	152.57	10	139.59
12	152.85	152.85	152.85	12	165.38	165.53	165.45	11	152.71
13	165.82	165.82	165.82	13	178.03	178.46	178.25	12	165.63
14	178.77	178.77	178.77	14	191.31	191.32	191.31	13	178.51
15	191.52	191.91	191.71	15	204.12	203.95	204.03	14	191.51
16	204.38	204.09	204.23	16	216.76	216.90	216.83	15	204.13
17	217.31	217.17	217.24	17	229.54	229.41	229.48	16	217.03
18	229.44	229.73	229.58	18	242.03	241.84	241.93	17	229.53
19	242.57	242.28	242.42	19	254.27	254.53	254.40	18	242.17
20	254.86	254.74	254.80	20	266.97	266.82	266.90	19	254.60
21	267.20	267.01	267.11	21	279.22	279.08	279.15	20	267.00
22	279.46	279.29	279.37	22	291.31	291.20	291.25	21	279.26
23	291.59	291.81	291.70	23	303.22	303.22	303.22	22	291.47
24	303.71	303.81	303.76	24	315.13	315.05	315.09	23	303.49
25	315.56	315.45	315.50	25	326.95	326.96	326.95	24	315.29
26	327.59	327.19	327.19	26	338.74	338.60	338.67	25	327.07
27	340.04	338.90	338.90	27	350.14	350.15	350.15	26	338.79
28	351.14	350.33	350.74	28	361.53	361.53	361.53	27	350.44
29	362.44	362.33	362.38	29	372.52	372.71	372.61	28	361.95
30	373.07	372.85	372.96	30	383.76	383.76	383.76	29	372.78
				31	394.69	394.91	394.80		
				32	405.28	405.59	405.44		
				33	416.14	415.92	416.03		

The combinations involving the upper state are the following:

$$\begin{aligned}
 R_1(J) - P_1(J) &= F_{1d}'(J+1) - F_{1d}'(J-1) = \Delta_2 F_{1d}'(J) \\
 {}^qR_{12}(J) - {}^oP_{12}(J) &= F_{1c}'(J+1) - F_{1c}'(J-1) = \Delta_2 F_{1c}'(J) \\
 R_2(J) - P_2(J) &= F_{2d}'(J+1) - F_{2d}'(J-1) = \Delta_2 F_{2d}'(J) \\
 {}^sR_{21}(J) - {}^qP_{21}(J) &= F_{2c}'(J+1) - F_{2c}'(J-1) = \Delta_2 F_{2c}'(J).
 \end{aligned}
 \tag{2}$$

These upper state combinations are tabulated in Table III. Large differences exist between the $\Delta_2 F_{1d}'(J)$ and $\Delta_2 F_{1c}'(J)$ values due to the large Λ -type doubling in the $\Pi_{1/2}$ state, while but small differences are noted between $\Delta_2 F_{2d}'(J)$ and $\Delta_2 F_{2c}'(J)$, corresponding to a small Λ -type doubling in the $\Pi_{1/2}$ state. However, for purposes of calculation of constants the average of each group (designated $\Delta_2 F_{dc}'$) is taken.

TABLE III. *Upper state combinations.* The $\Delta_2 F'$ headings are defined by Equations (2). $\Delta_2 F_{1d'}(J)$ is the average of $\Delta_2 F_{1c}(J)$ and $\Delta_2 F_{1d}(J)$. Likewise, $\Delta_2 F_{2dc'}(J)$ is average of $\Delta_2 F_{2d'}(J)$ and $\Delta_2 F_{2c'}(J)$. The values marked p involve perturbed levels, and are therefore not included in the averages.

$J'' + \frac{1}{2}$	$\Delta_2 F_{1d'}(J)$	$\Delta_2 F_{1c}(J)$	$\Delta_2 F_{1d}(J)$	$J'' + \frac{1}{2}$	$\Delta_2 F_{2d'}(J)$	$\Delta_2 F_{2c'}(J)$	$\Delta_2 F_{2dc'}(J)$
2	26.87			3		42.72	
3	40.49			4	56.51	55.80	56.16
4	54.26			5	70.35	70.03	70.19
5	68.01	69.46	68.73	6	84.10	84.26	84.18
6	81.59	82.95	82.27	7	98.28	98.22	98.25
7	95.41	96.85	96.13	8	112.14	112.07	112.10
8	109.16	110.79	109.98	9	125.94	125.91	125.95
9	123.06	124.40	123.73	10	139.85	139.72	139.78
10	136.19	137.90	137.05	11	156.14 p	153.66	153.66
11	149.88	151.41	150.65	12	168.20 p	167.17	167.17
12	163.29	164.83	164.06	13	178.84 p	180.92	180.92
13	176.60	178.19	177.39	14	194.50	194.56	194.53
14	189.81	191.29	190.55	15	208.00	208.03	208.01
15	203.25	204.67	203.96	16	221.58	221.63	221.61
16	216.39	217.74	217.07	17	234.80	234.29	234.54
17	229.44	230.71	230.13	18	247.90	247.84	247.87
18	242.74	243.95	243.45	19	261.11	260.92	261.01
19	255.49	256.86	256.17	20	274.11	274.03	274.07
20	268.41	269.65	269.03	21	287.26	286.81	286.54
21	281.17	282.22	281.70	22	299.99	299.58	299.78
22	293.76	294.81	294.28	23	312.56	312.26	312.41
23	306.24	307.23	306.74	24	325.02	324.71	324.87
24	318.62	319.67	319.15	25	337.56	337.48	337.52
25	331.13	331.72	331.43	26	349.76	349.74	349.75
26	343.64	344.11	343.87	27	362.00	361.46	361.74
27	355.53	356.39	355.96	28	373.80	373.43	373.61
28	367.66	367.88	367.77	29	385.90	385.23	385.57
29	379.40	379.87	379.63	30	397.27	397.58	397.42
30	390.99	391.11	391.05	31	408.54		408.54
31		402.43		32	420.19		420.19
				33	431.19		431.19
				34	442.38		442.38
				35	452.78		452.78

EVALUATION OF CONSTANTS B , D , AND A

The energy equation⁵ for the terms of the normal $^2\Sigma$ state, which is typical case b , is

$$T(J) = T_0^e + T^v + B''[K(K+1) + G^2] + \gamma''[J(J+1) - K(K+1) - S(S+1)] + D''K^2(K+1)^2$$

with $S = \frac{1}{2}$.

Representing by $T_1(K)$ the states with $J = K + S$ and by $T_2(K)$ the states with $J = K - S$, it is easily seen that $T(K) = \frac{1}{2}\{T_1(K) + T_2(K)\}$ is given by the equation

$$T''(K) = T_0^e + T^v + B''[K(K+1) - G^2] + D''K^2(K+1)^2 + S\gamma$$

from which one obtains

$$\Delta_2 F''(K) = B''(4K+2) + D''(8K^3 + 12K^2 + 12K + 4). \quad (3)$$

The application of this equation to the experimental values given in the last column of Table II yields the B'' and D'' given in Table IV.

⁵ R. S. Mulliken, Rev. Mod. Phys. 2, 106-107 (1930).

TABLE IV. Constants resulting from the analysis of the ${}^2\Pi \rightarrow {}^2\Sigma$ (0, 0) band of BaH (cm^{-1} units).

$B_0'' = 3.404$	$D_0'' = -9.61 \times 10^{-5}$
$B_{0,-1/2}' = 3.4468$	$D_{0,-1/2}' = -1.13 \times 10^{-4}$
$B_{0,+1/2}' = 3.5156$	$D_{0,+1/2}' = -1.20 \times 10^{-4}$
${}^2\Sigma$ state: $\gamma_0 = +0.186, r_0'' = 2.22 \times 10^{-8}$ cm	
${}^2\Pi$ state: $p_0 = +0.85, q_0 = +0.0067, A = 462$.	

The term values for the ${}^2\Pi$ state may be represented by an equation which Mulliken and Christy⁶ have adopted from Van Vleck's⁷ theoretical paper on Λ -type doubling. This equation takes into account the effects of spin and Λ -type doubling, and if $|A| \ll |\nu(\Pi, \Sigma)|$ may be written

$$T(J) = T_0 + B_v \left\{ (J + \frac{1}{2})^2 - 1 \pm \frac{1}{2}X \right\} + \frac{1}{2} \left\{ o + \frac{1}{2}p^* + q^*(J + \frac{1}{2})^2 \right\} \\ \pm \frac{1}{2}X^{-1} \left\{ (2 - Y)(o + \frac{1}{2}p^* + q^*) + (p^* + 2q^*)(J - \frac{1}{2})(J + 1\frac{1}{2}) \right\} \\ + [\pm \frac{1}{2}(J + \frac{1}{2})] \left\{ [\pm 1 + X^{-1}(2 - Y)](\frac{1}{2}p + q) + 2X^{-1}q(J - \frac{1}{2})(J + 1\frac{1}{2}) \right\} \\ + D(J + \frac{1}{2})^4.$$

For the meaning of all terms reference should be made to Mulliken and Christy's paper. As to the signs, whenever the sign \pm occurs the upper sign refers to T_2 states and the lower sign to T_1 states, while whenever the bracketed sign $[\pm]$ occurs the $+$ sign refers to T_d levels and the $-$ sign to T_c levels.

If we take the average of $T_d(J)$ and $T_c(J)$ the third line in the above equation disappears, since one would involve the $+$ sign and the other the $-$ sign. Hence, the average energy term $T_{dc}(J) = \frac{1}{2} \{ T_d(J) + T_c(J) \}$ becomes

$$T_{dc}(J) = T_0 + J(J + 1) \left[B_v \pm \frac{B_v^2}{A} + \frac{q^*}{2} \pm \frac{p + 2q}{2X} \right] + D[J^2(J^2 + 1)]$$

+ (terms independent of J or the J involved in X terms).

Setting

$$B_{\Sigma}^* = \left[B_v + \frac{q^*}{2} \pm \left(\frac{B_v^2}{A^2} + \frac{p + 2q}{2X} \right) \right]$$

with \pm sign according as $\Sigma = \pm \frac{1}{2}$, one obtains the customary form of $\Delta_2 F$ equation:

$$\Delta_2 F_{dc}(J) = B_{\Sigma}^*(4J + 2) + D_{\Sigma}'(8J^3 + 12J^2 + 12J + 4). \quad (4)$$

Applying this equation to the average $\Delta_2 F_{dc}(J)$'s given in Table III, the B' and D' values given in Table IV were obtained.⁸

The coupling constant A is determined in the usual way from the Hill and Van Vleck equation

$$T_0 = T_0^e + G(v) + B_v \left\{ (J + \frac{1}{2})^2 - \Lambda^2 \pm \frac{1}{2} [4(J + \frac{1}{2})^2 - 4A^2\Lambda^2/B + A^2\Lambda^2/B_v^2] \right\}.$$

By taking the difference of two band frequencies, one near each origin, which have the same lower state but arise from different upper states, one of

⁶ R. S. Mulliken and A. Christy, Phys. Rev. **38**, 87 (1931).

⁷ J. H. Van Vleck, Phys. Rev. **33**, 406 (1929).

⁸ Computation of $B_{0,-1/2}$ with the $\Delta_2 F_{1c}(J)$ and $\Delta_2 F_{1d}(J)$ values of Table III separately gives 3.4762 and 3.4175 respectively. The $B_{0,-1/2} = 3.4468$ given in Table IV is the mean of these two values.

which is a T_1 state and the other a T_2 state, a quadratic equation in A and B is obtained. By selecting, then, another suitable pair of frequencies a second equation is evaluated, and A can be found by solving the two equations simultaneously. The average of a number of such determinations has led to the value $A = 462$ as given in Table IV.⁹ This value of A is much smaller than the A expected from the value 832 of the corresponding L, S coupling of the lowest 3P state of Ba (*cf.* discussion below).

SPIN AND Λ -TYPE DOUBLING

It is of interest to investigate the spin and Λ -type doubling in bands because of the light thus thrown on the probable electron configurations of the molecular states involved. The theoretical work of Van Vleck⁷ has been interpreted in a detailed paper by Mulliken and Christy⁶ with applications to many known band systems. The spin doubling is defined by $\Delta\nu_{12}(K) = T_1(K) - T_2(K)$;—the separation of T_1 and T_2 levels having the same K value. Theoretically,

$$\Delta\nu_{12}(K) = \gamma(K + \frac{1}{2}) \quad (5)$$

experimentally it is determined from the separation of the corresponding lines in P_1 and $^PQ_{12}$, Q_1 and $^Q R_{12}$, $^Q P_{21}$ and Q_2 , and $^R Q_{12}$ and R_2 branches with the same K .

The Λ -type doubling is defined as $\Delta\nu_{dc}(J) = T_d(J) - T_c(J)$;—the separation of T_d and T_c levels with the same J . Theoretically, for case $a\Delta\nu_{dc}(J) = -p(J + \frac{1}{2})$ for a $^2\Pi_{1/2}$ state and

$$\Delta\nu_{dc}(J) = \left(\frac{p}{Y^2} + \frac{2q}{Y} \right) (J - \frac{1}{2})(J + \frac{1}{2})(J + 1\frac{1}{2})$$

for a $^2\Pi_{11/2}$ state; experimentally, the Λ -type doubling is obtained from the relation

$$\Delta\nu_{dc}(J + \frac{1}{2}) = \frac{1}{2} \{ [R(J) - Q(J)] - [Q(J + 1) - P(J + 1)] \}. \quad (7)$$

Figure 2 shows the spin and Λ -type doubling for these BaH states. Each point on the spin doubling curve is the average of the four values obtained. The curve varies linearly with $(K + \frac{1}{2})$ as expected, the slope giving the value of γ listed in Table IV. The Λ -type doubling in the $^2\Pi_{1/2}$ state is large and negative, while in the $^2\Pi_{11/2}$ state it is small and positive. It is interesting to note that the doubling in the $^2\Pi_{11/2}$ state is practically zero until the perturbed level is reached, from which point it appears to increase as shown. The values of p and q calculated from equations (6) are given in Table IV.

⁹ Theoretically, A could be determined from the values of B_{Σ^*} . For instance, the value X could be assumed to have value Y for low J 's since the value of Y is large ($Y = A/B = 125$). Thus $B_{\Sigma^*} = B_v + q \pm 1/A [B_v^2 + B_v^*(p + 2q/2)]$ where p and q have the values given in Table IV. Actual calculation by this method gives $A = 395$, which is much lower than the best value 462. The disagreement is due to (1) approximations made in obtaining B_{Σ} and (2) slight errors in B_{Σ^*} causing a large error in constants (for example, a difference of 0.01 in B^* causes a difference of 70 in A).

The effect of Λ -type doubling on the relative position of the four levels of the ${}^2\Pi$ state as K' increases is shown in Fig. 3. All term values are calculated with $T_{1d}(J)$ assumed equal to zero; the separation of T_{1c} and T_{1d} levels is obtained directly from $\Delta\nu_{dc}(J)$ values for the ${}^2\Pi_{1/2}$ state; T_{2d} is computed from the difference in wave number of the lines $P_2(J) - {}^PQ_{12}(J) = T_{2d}(K') - T_{1d}(K')$ where $K' = J'' + \frac{1}{2}$; and finally, T_{2c} values are obtained from $T_{2d} + \Delta\nu_{dc}(J)$ for the ${}^2\Pi_{1/2}$ state, using however the interpolated values of $\Delta\nu_{dc}(J)$ for the actual K' level.

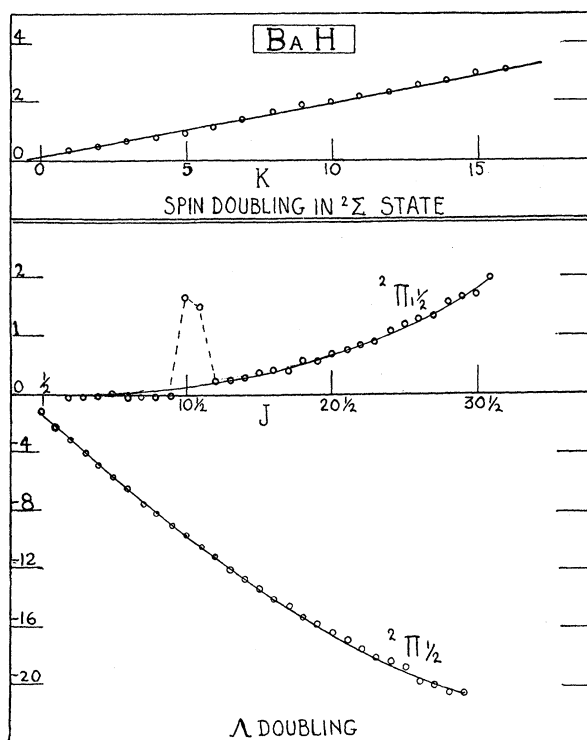


Fig. 2. Spin doubling in the normal ${}^2\Sigma$ state and Λ -type doubling in the ${}^2\Pi$ state of BaH. The linear doubling relation for the ${}^2\Sigma$ state is apparent. Note that the Λ -type doubling is large in the ${}^2\Pi_{1/2}$ levels, while it is small and of opposite sign in the ${}^2\Pi_{3/2}$ levels. The irregularity in the ${}^2\Pi_{1/2}$ curve is due to the perturbation caused by some lower-lying excited level of BaH.

Comparison of Fig. 3 with similar graphs for SrH (Fig. 3 in following paper) and CaH¹⁰ brings out certain interesting features. In BaH the T_{1c} levels are above the T_{1d} levels while the T_{2c} levels are below the T_{2d} . The opposite is true for SrH and for low K values for CaH. The doubling in the ${}^2\Pi_{1/2}$ state is very small indeed, as predicted for case a by Van Vleck's theory, while the increase of doubling in the corresponding state of SrH and CaH shows that each in turn approaches closer to case b with increase in the molecular rotation. Also, the ${}^2\Pi_{1/2}$ level separations should be large for case a but

¹⁰ Reference 6, p. 117.

should decrease and finally change sign as case *b* is approached. It is observed that in BaH these levels do not begin this tendency toward case *b*—even at the highest *K* we have observed, while the SrH level does start bending back at $K'=28$, and for CaH it starts back at $K'=6$, passing through zero at $K'=11$.

Mulliken and Christy⁶ have shown that Van Vleck's case of "pure precession", or something closely akin to it, exists between some of the known states of most diatomic molecules. In this case at least one electron has a well-defined *l* shared between say a Π state with $\lambda=1$ and a Σ state with $\lambda=0$. Then the γ , p , q constants have the following values

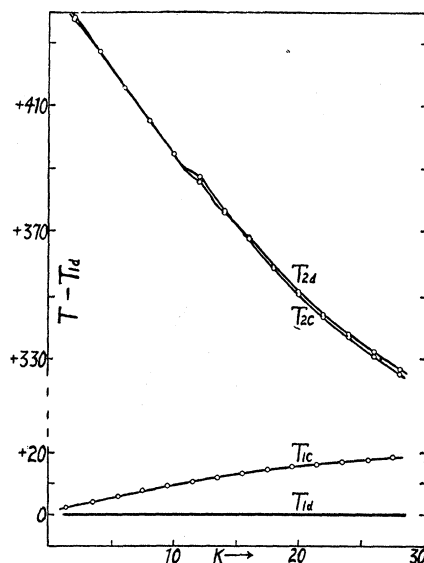


Fig. 3. Relative position of levels in the ${}^2\Pi$ state of BaH. The doublet interval $T_{2d}-T_{2c}$ is very small, since the coupling is strictly case *a*. And for the same reason there is no tendency observable up to $J=30\frac{1}{2}$ for the T_1 levels to begin to come together.

$$\gamma = p = 2AB_v l(l+1)/\nu(\Pi, \Sigma)$$

and

$$q = 2B_v^2 l(l+1)/\nu(\Pi, \Sigma) \quad (8)$$

where *A*, *B*, and *l* have their usual meaning, and $\nu(\Pi, \Sigma)$ is the wave number difference of the Π and Σ states which have the common *l*. This $\nu(\Pi, \Sigma)$ is positive or negative as Π is higher or lower than Σ .

The disagreement between the observed γ and *p* values for the normal ${}^2\Sigma$ and this ${}^2\Pi$ state of BaH leads to the conclusion that the case of pure precession does not exist between these two states. Hence, since these states do not have a common *l* they must arise from different electronic configurations. But from the sign and magnitude of *p* and *q* and the calculated values of *A* and *B*, computation with Eq. (8) with $l=1$ leads to the conclusion that a

case of pure precession does exist between the known ${}^2\Pi$ state and an unknown excited ${}^2\Sigma^+$ state some 7000 wave numbers below the ${}^2\Pi$ state. Unfortunately a band system arising from a transition from this predicted ${}^2\Sigma$ state to the normal ${}^2\Sigma$ state of BaH would lie too far into the infrared to be photographed. This may be the state a level of which is causing the perturbation observed at $J=11\frac{1}{2}$ in the ${}^2\Pi_{1/2}$ state.

DISCUSSION

The probable electron configuration of the BaH molecule in these states is not as readily determined as for the other similar hydride molecules. As Mulliken and Christy have pointed out, the fact that for CaH the observed p_0 and q_0 constants of the ${}^2\Pi$ state and the γ_0 for the doubling in the upper ${}^2\Sigma$ state indicate clearly that these two states have a relation of pure precession between them with $l=1$ makes it very probable that these two states of CaH are $\dots 4p\pi$ and $\dots 4p\sigma$. The normal ${}^2\Sigma$ state of CaH may then possibly be $\dots 3d\sigma$, since in the Ca atom the $3d$ electron is almost as firmly bound as the $4p$. In SrH, as is shown in the following paper, an almost identical arrangement of levels is found. For BaH also, as has been demonstrated, there exists no pure precession relation between the ${}^2\Pi$ and the normal ${}^2\Sigma$ states. But there is the evidence cited that interaction does occur between the ${}^2\Pi$ state and an excited ${}^2\Sigma^+$ state below it. The fact that this ${}^2\Sigma$ state lies below the ${}^2\Pi$ is just what one would normally expect if they are really $\dots 6p\sigma$ and $\dots 6p\pi$ respectively.

This ${}^2\Pi$ BaH state is unique among the corresponding ${}^2\Pi$ states of these hydrides of the elements in the second column of the periodic table, however, in having its coupling constant A for the S, Λ interaction differing very considerably from the A for the lowest 3P level of the atom concerned. Now Ba is the only one of these atoms for which the lowest 3D level is *below* the lowest 3P level, the interval being 0.41 volt. It may be that in the formation of the BaH molecule, these two atomic levels are forced together and combine to form the molecular ${}^2\Pi$ state with this lowered A constant. The dissociation relations would then be quite complicated. It is unfortunate that the indicated bands farther into the red cannot be investigated in order to note the interaction existing between their upper state and this "hybrid" ${}^2\Pi$ state.

We wish to thank Dr. Alden J. King for the supply of pure barium presented to us for this research, and we are indebted to Professor R. S. Mulliken for helpful discussion on the subject of electron configurations.

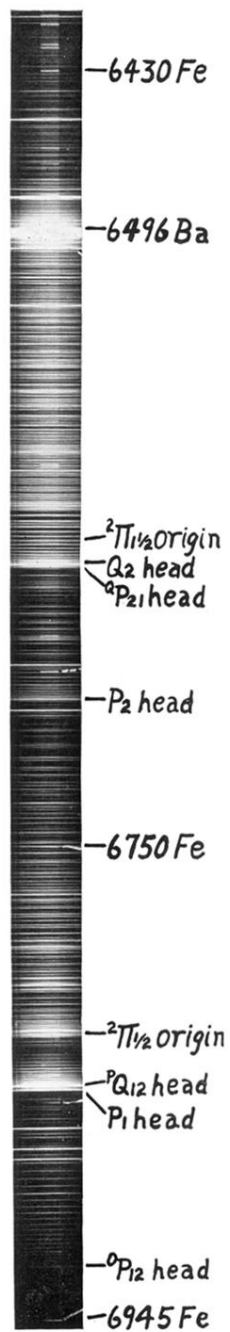


Fig. 1. Reproduction of the ²II, ²Σ BaH band lying between 6380Å and 6925Å. Note the considerable spacing between the heads of the satellite and main branches, and their equal intensity.